archives
of thermodynamics
Vol. **39**(2018), No. 2, 55–72
DOI: 10.1515/aoter-2018-0012

Impact of subgrid modelling and numerical method on autoignition simulation of two-phase flow

JAKUB STEMPKA*

Czestochowa University of Technology, Institute of Thermal Machinery, Faculty of Mechanical Engineering and Computer Science, Armii Krajowej 21, 42-201 Czestochowa, Poland

Abstract The present work focuses on analyses of the autoignition delay time predicted by the large eddy simulation (LES) method by applying different subgrid scales (SGS) models and two different discretization schemes. The analysed flow configuration is a two-phase chemically reacting turbulent flow with monodispersed evaporating fuel droplets. The impact of numerical procedure is investigated in a 3D flow domain with a temporally evolving mixing layer that constituted between the streams of fuel and oxidizer that moved in opposite directions. The upper stream of cold gas carries a dispersed fuel spray (ethanol at 300 K). The lower stream is a hot air at 1000 K. Three commonly used in LES, SGS models are investigated, namely: classical Smagorinsky model, model proposed by Vreman and the σ-model proposed by Nicoud. Additionally, the impact of two discretization schemes, i.e., total variation diminishing (TVD) and weighted essentially nonoscillatory (WENO) is analysed. The analysis shows that SGS model and discretization scheme can play a crucial role in the predictions of the autoignition time. It is observed that for TVD scheme the impact of SGS model is rather small. On the contrary, when the WENO scheme is applied the results are much more dependent on the SGS model.

Keywords: Discretization schemes; Convective terms; WENO; TVD; Spray combustion

*Email: stempka@imc.pcz.pl

Nomenclature

A	–	velocity gradient tensor
B	–	Spalding number
c	–	specific heat capacity, J/kg K
C	–	model constant
D	–	differential operator
DNS	–	direct numerical simulation
$G_\Delta(\cdot)$	–	convolution kernel of the spatial filter
h	–	specific enthalpy, J/kg
J	–	turbulent diffusion flux
k	–	wave number, 1/m
L	–	enthalpy of vaporization, J/kg
LES	–	large eddy simulation
Le	–	Lewis number
m	–	mass, kg
$\dot{m}$	–	mass flux, kg/s
Nu	–	Nusselt number
p	–	absolute pressure, Pa
r	–	radius, m
RANS	–	Reynolds averaged Navier-Stokes equations
Re	–	Reynolds number
S	–	rate of strain tensor
Sc	–	Schmidt number
SGS	–	subgrid scale model
Sh	–	Sherwood number
T	–	temperature, K
T_i	–	turbulence intensity, %
t	–	time, s
u, v, w	–	velocity component, m/s
Y	–	mass fraction of a species
x, y, z	–	Cartesian coordinates

Greek symbols

δ	–	shear layer thickness, m
Δ	–	spatial filter size, m
η	–	length scale, m
λ	–	Taylor microscale, m
υ	–	subgrid scale turbulent viscosity, m^2/s
ρ	–	density, kg/m^3
σ	–	turbulent Prandtl number
σ_{ij}	–	viscous stress tensor
τ	–	deviatronic part of the subgrid scale tensor/relaxation time
$\phi(y)$	–	smoothing function
$\overline{\dot{\omega}}$	–	chemical source term

Subscripts

g	–	gas phase
h	–	enthalpy in source term
i, j	–	ith, jth direction
k	–	kth species
K	–	Kolmogorov length scale
l	–	liquid phase
m	–	momentum in source term/model constant
$mass$	–	mass in source term
p	–	particle
s	–	surface
Y	–	species in source term

Superscripts

$\tilde{\cdot}$	–	density weighted quantity
$\bar{\cdot}$	–	filtered quantity
$\cdot'$	–	signal RMS
sgs	–	subgrid scale

1 Introduction

Analyses of systems utilizing multiphase turbulent combustion processes lead to advancements of practical devices regarding both, improvements of efficiency and reduction of pollutants production, e.g., circulating fluidized beds [23], diesel engines with reheat systems [24], power plants utilizing the oxy-combustion [25] and many others. Particularly, operation of diesel engines consists of various phenomena such as: spray injection and atomization droplets evaporation, formation of combustible gaseous fuel and chemical reactions. These processes are influenced by the local and global properties of the gaseous continuous phase. These factors make their experimental investigations very difficult or even impossible. Fortunately, with a quick development of high-performance computers the analyses of combustion in two-phase flows are possible via numerical simulations. However, their usefulness is limited by the accuracy of models and methods applied. Such models require validation against the experimental data from variety of different flow configurations, since the empirical studies are limited and the availability of experimental data is rather poor. This makes the numerical analyses a very important research field. For many cases they are the only source of information, and therefore, it is important to be aware of their limitations in different applications.

Numerical simulation of turbulent combustion with fuel spray is an extremely complicated task, since the transient phenomena characterized by

the time and spatial-scales that differ in several orders of magnitude need to be considered. Simulations of multiphase turbulent combustion in the presence of droplet laden gaseous media are based mainly on two modelling approaches, namely: direct numerical simulations (DNS) [4,5] and large eddy simulations (LES) [6–8,11]. The former approach does not require the subgrid side (SGS) models to be used since it resolves all the flow scales. However, due to the high computational cost, it is limited mainly to flows with relatively low Reynolds numbers. The LES is less expensive than DNS because it can be applied on computational meshes much coarser than that required for DNS. This significantly reduces the simulation effort especially for very complex flows. The LES approach uses models based on simplified assumptions but is undoubtedly useful in many problems of practical importance. However, it still needs to be thoroughly tested and validated when applied for modelling of new flow configurations. Compared to very accurate but computationally expensive DNS, the LES can be regarded as an accurate approach for computations of the large flow scales. In the LES due to the filtering procedure additional unclosed terms are introduced. These account for the contribution of unresolved scales and need to be modelled. Small scales are relatively easy to model since they are homogenous and weakly affected by the boundary conditions compared to the larger ones [9]. In the paper three different SGS models have been analysed, namely: Smagorinsky [1], Vreman [2] and σ-model [3].

In the current work the comparative numerical study of the influence of subgrid modelling and discretization schemes on the autoignition delay in turbulent and reacting two-phase flow was undertook. The numerical models used in the computations are characterized in the following sections. The computations were performed using an academic 3D high-order compact difference LES solver SAILOR [13]. The impact of the SGS models along with different discretization schemes for convective terms (WENO and TVD) used during the simulations was assessed. The differences in the autoignition delays, predicted by different numerical SGS models and discretization schemes were compared and discussed in the results section.

2 Mathematical model

2.1 LES transport equations

Large eddy simulation is based on a separation of scales of the fluid motion into large and small ones. The governing equations are spatially filtered

based on an assumed spatial filter size, Δ, and the kernel filter function, G. The spatial filtering is defined as: $\bar{f} = G * f$, where $*$ stands for the convolution operation. In variable density flows the Favre-filtering is usually applied and it is defined as [9]

$$\tilde{f} = \frac{\overline{\rho f}}{\bar{\rho}} \, . \tag{1}$$

For incompressible low Mach number two-phase flows with chemical reactions the filtered set of equations is given as [9,12]

$$\frac{\partial \bar{\rho}}{\partial t} + \frac{\partial \bar{\rho} \tilde{u}_j}{\partial x_j} = \bar{\dot{S}}_{mass} \, , \tag{2}$$

$$\frac{\partial \bar{\rho} \tilde{u}_i}{\partial t} + \frac{\partial \bar{\rho} \tilde{u}_i \tilde{u}_j}{\partial x_j} = -\frac{\partial \bar{p}}{\partial x_i} + \frac{\partial \bar{\sigma}_{ij}}{\partial x_j} + \frac{\partial \tau_{ij}^{sgs}}{\partial x_j} + \bar{\dot{S}}_m \, , \tag{3}$$

$$\frac{\partial \bar{\rho} \tilde{Y}_k}{\partial t} + \frac{\partial \bar{\rho} \tilde{Y}_k \tilde{u}_j}{\partial x_j} = \frac{\partial}{\partial x_j} \left[\left(\frac{\mu}{\sigma} + \frac{\mu_{sgs}}{\sigma_{sgs}} \right) \frac{\partial \tilde{Y}_k}{\partial x_j} \right] + \bar{\dot{S}}_Y + \bar{\omega}_k \, , \tag{4}$$

$$\frac{\partial \bar{\rho} \tilde{h}}{\partial t} + \frac{\partial \bar{\rho} \tilde{h} \tilde{u}_j}{\partial x_j} = \frac{\partial}{\partial x_j} \left[\left(\frac{\mu}{\sigma} + \frac{\mu_{sgs}}{\sigma_{sgs}} \right) \frac{\partial \tilde{h}}{\partial x_j} \right] + \bar{\dot{S}}_h \, . \tag{5}$$

The symbols $\bar{\sigma}_{ij}$, ρ, u, p, μ and h are the viscous stress tensors of the resolved field: density, velocity, pressure, molecular viscosity and enthalpy of the gas phase. The deviatronic part of the subgrid stress tensor τ_{ij}^{sgs} need to be modelled and in the current work it is computed using three different models described in detail in the Subsec. 2.4. The terms $\bar{\dot{S}}_{mass}^{\alpha}$, $\bar{\dot{S}}_{Y}^{\alpha}$, $\bar{\dot{S}}_{m,}^{\alpha}$, $\bar{\dot{S}}_{h}^{\alpha}$ stand for source terms that couple the dispersed phase with the flow field. The σ is the turbulent Prandtl or conversely the Schmidt number, since Lewis number was set to be unity. The value Le = 1 was used to simplify the analyses and modelling approach similarly to other authors [4,11]. In most cases when the spray evaporates in air, it creates very lean mixtures, and therefore, the differences between diffusivities of the species play a minor role. The symbol $\tilde{Y}_k$ represents a k-th species density-weighted mass fraction. The symbol $\bar{\omega}_k$ appearing in Eq. (4) is a chemical source term. Here its computation is performed based on the filtered values as in the implicit LES (ILES) approach of Duwig *et al.* [6]. Such a strategy does not require modelling of subgrid scales impact on a reaction term, but the subgrid viscosity is modelled exactly as in classical LES approach.

2.2 Dispersed phase model

The source terms in Eq. (6)–(8) are formulated as in [11] while their computation is performed by a summation over the αth droplet located in the computational grid cells:

$$\bar{\dot{S}}^{\alpha}_{mass} = \bar{\dot{S}}^{\alpha}_{Y} = -\frac{1}{V}\sum_{\alpha=1}^{N_p}\frac{dm_p^{(\alpha)}}{dt}\ , \tag{6}$$

$$\bar{\dot{S}}^{\alpha}_{m,} = -\frac{1}{V}\sum_{\alpha=1}^{N_p}\frac{d(m_p v_p)^{(\alpha)}}{dt}\ , \tag{7}$$

$$\bar{\dot{S}}^{\alpha}_{h} = -\frac{1}{V}\sum_{\alpha=1}^{N_p}\left(c_p m_p\frac{T_g - T_p}{\tau_c} + \frac{dm_p}{dt}h_v\right)^{(\alpha)}\ . \tag{8}$$

The symbol V denotes the volume of computational grid cell in which the droplet is located, m_p is a droplet mass, v_p – the droplet velocity, c_p – the liquid fuel heat capacity, T_g and T_p are the temperature of gaseous medium at the droplet position and droplet temperature, respectively, h_v denotes the enthalpy evaporated fuel.

The dispersed phase model is based on the Lagrangian description. In such a representation each fuel droplet is tracked individually. Droplet-gas interactions are coupled with the continuous phase which is expressed in the classical Eulerian coordinates. The procedure implemented is similar to the one proposed by Maxey and Riley [14], except the stochastic term which is not considered. The equations of motion for droplets are defined as follow:

$$\frac{dx_p}{dt} = v_p \tag{9}$$

and the droplet velocity is computed from:

$$\frac{dv_p}{dt} = \frac{\tilde{u} - v_p}{\tau_p}\ , \tag{10}$$

where $\tilde{u}$ is the gas phase velocity at the droplet's position. The symbol τ_p represents a relaxation time

$$\tau_p^{-1} = \frac{3}{8}\frac{\rho}{\rho_l}C_D\frac{|\tilde{u} - v_p|}{r_p} \tag{11}$$

in which ρ_l is a liquid fuel density, r_p represents the particle radius and C_D the particle drag coefficient for spherical droplets.

2.3 Evaporation model

A single component, isolated droplet evaporation model based on the Spalding formulation [15] was implemented into the code. The droplet mass changes according to

$$\frac{dm_p}{dt} = \dot{m} = \pi D_p \left(\frac{k}{c_p}\right)_g \mathrm{Sh} \ln\left(1 + B_M\right) \ , \tag{12}$$

where m_p is the droplet mass, D_p, denotes the droplet diameter, and Sh stands for the Sherwood number. It is expressed in terms of the Reynolds number, Re, and the Schmidt number, Sc, and is given as [26]

$$\mathrm{Sh} = \frac{1 + 0.276\mathrm{Re}^{0.5}\mathrm{Sc}^{0.33}}{\left(1 + \frac{1.232}{\mathrm{ReSc}^{1.33}}\right)^{0.5}} \ . \tag{13}$$

For computing the droplet surface temperature, the model of Abramzon and Sirignano [16] was incorporated into the code. The model has the following form:

$$m_p c_p \frac{dT_p}{dt} = \dot{m}\left[\frac{c_{p,g}(T_\infty - T_p)}{B_T} - L\right] \ , \tag{14}$$

where $c_{p,g}$ is the specific heat capacity of a gas-vapour mixture, L is the fuel latent heat of vaporization, and B_T is the Spalding heat transfer number.

2.4 Subgrid scale turbulent viscosity models

The intention of the current work was to apply and compare different SGS models. The modelling procedure is based on an appropriate closure for SGS turbulent viscosity υ_{sgs} which has a general form

$$\upsilon_{sgs} = \left(C_m \Delta\right)^2 D_m(\bar{u}) \tag{15}$$

in which C_m is the model constant, Δ is the spatial filter size, and D_m is a differential operator associated with the model acting on the resolved velocity field $\bar{u}$[1–3]. The turbulent viscosity is used to model the subgrid stress tensor $\tau_{ij}^{sgs} = -2\upsilon_{sgs}\rho S_{ij}$, where S_{ij} is the strain rate tensor of the filtered velocity field defined as $S_{ij} = 1/2\left(\partial u_i/\partial x_j + \partial u_j/\partial x_i\right)$.

Well known classical Smagorinsky model [1] was used in computations

among other. It is based on the assumption that small scale energy production and dissipation are in balance. It has the following form:

$$\upsilon_{sgs} = (C_s \Delta)^2 \, |\bar{S}| \tag{16}$$

in which $|S| = \sqrt{2 S_{ij} S_{ij}}$ and the model constant was set to $C_s = 0.1$. The major drawback of this model is that the differential operator does not vanish in near-wall regions. Overall the model is very simple and computationally inexpensive and hence is broadly used.

In general, a reliable turbulence model should ensure that the eddy viscosity tends toward zero when approaching the laminar and transitional regions. This is not satisfied in the classical Smagorinsky model. On the contrary the model proposed by Vreman meets this criterion very well. In this case the SGS eddy viscosity vanishes in near-wall regions and the model is defined through the subgrid viscosity as

$$\upsilon_{sgs} = C_v \sqrt{\frac{Q_G}{\bar{A}_{ij} \bar{A}_{ij}}} \, , \tag{17}$$

where $\bar{A}_{ij} = \frac{\partial \bar{u}_i}{\partial x_j}$ and $Q_G = 1/2 \left[G_{kk}^2 - G_{ij} G_{ji} \right]$ are the resolved velocity gradients and the second invariant of the tensor in which $G_{ij} = \Delta^2 \bar{A}_{ik} \bar{A}_{jk}$. The model constant was set to $C_v = 0.025$. The Vreman's model was found to be more accurate than Smagorinsky model in LES of inhomogeneous turbulence and in channel flows [2].

The third SGS eddy viscosity model considered in the analysis presented in this study is called the σ-model and it was proposed by Nicoud *et al.* [3,19]. Its formulation promotes the near-wall scaling and vanishing [19] due to the turbulence dumping properties of the no-slip condition, similarly to the Vreman's model. The σ-model however is based on the singular value decomposition (SVD) procedure applied to velocity gradient tensor $\frac{\partial u_i}{\partial x_j}$ to construct an improved differential operator for SGS turbulent viscosity. It consists of the three singular values of the velocity gradient tensor $\sigma_1 \geq \sigma_2 \geq \sigma_3 \geq 0$. The σ-model and the associated differential operator is formulated as

$$\upsilon_{sgs} = (C_\sigma \Delta) \, D_\sigma \, , \tag{18}$$

where the differential operator is defined as $D_\sigma = \frac{\sigma_3 (\sigma_1 - \sigma_2)(\sigma_2 - \sigma_3)}{\sigma_1^2}$ and the model constant is equal to $C_\sigma = 0.1$. As shown in [19] the σ-model presents superior characteristics over the model of Smagorinsky and turned out to be slightly better than the model of Vreman.

3 Case setup

Analysed domain that is shown in Fig. 1 consists of the two streams of fluid that are moving in opposite directions, providing the temporal shear-layer evolution. The upper part is a droplet-laden stream of cold air ($T = 300$ K) which carries the fuel spray (ethanol). The lower part of the domain is filled by a hot oxidizer (air) at temperature equal to $T = 1000$ K. The constant temperature boundary conditions are defined on the upper and lower wall and the temperatures were set to 300 K and 1000 K respectively. The computational domain is characterized by the following dimensions: $L_y = 0.04$ m $L_x = 0.025$ m and $L_z = 0.01$ m.

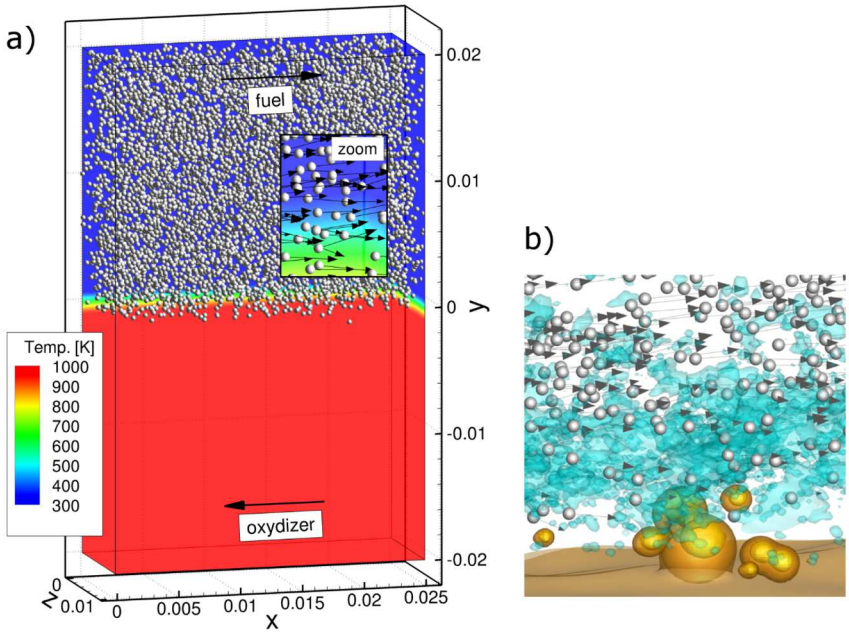

Figure 1: Representation of the computational domain showing: a) the initial temperature distribution and b) isosurfaces of high temperatures revealing autoignition spots and isosurfaces of fuel mass fraction $Y_F = 0.03$ (light blue colour) at a later time of simulation. The fuel droplets are represented by white spheres and vectors showing their velocities.

The domain was periodic in the y-normal and z-normal directions. The computational grid consisted of 256 nodes in streamwise (x) direction, 128 nodes in transversal (y) direction and 64 nodes cells in spanwise (z) di-

rection. It resulted in following grid spacings in (x), (y), and (z) directions respectively: $\Delta x = 9.77 \times 10^{-5} m$, $\Delta y = 3.13 \times 10^{-4}$ m, and $\Delta z = 1.56 \times 10^{-4}$ m.

In the current analysis the fuel is assumed to be in a dilute regime. Therefore, the modelling of droplet-droplet interaction is omitted without serious inaccuracies. Fuel droplets initially have a uniform size equal to 100 μm and the overall fuel mass is $0.000396\,g$. Considering the total volume of the domain it gives a fuel volume fraction of 10^{-4}.

For each case the pseudo-turbulent velocity field characterized by the specified initial turbulence intensity and the velocity RMS (the root mean square of the speed) is superimposed. The turbulence field was previously computed in an external spectral generator based on assumed kinetic energy spectrum, defined according to the formula

$$E(k,y) = \phi(y) 16 \sqrt{\frac{2}{\pi}} \frac{u'^2}{k_0} \left(\frac{k}{k_0}\right)^4 \exp\left[-2\left(\frac{k}{k_0}\right)^2\right] \ . \tag{19}$$

The $u' = \left\langle \sqrt{u'u'} \right\rangle$ is a root mean square of the initial velocity fluctuations and k_0 is an adjustable wave number used to generate the turbulent flow field with arbitrary chosen length of the Taylor microscale defined as $\lambda = \langle u'^2 \rangle^{1/2} \Big/ \left\langle (\partial u/\partial x)^2 \right\rangle^{1/2}$. The imposed streamwise velocity profile across the mixing layer is defined by a hyperbolic tangent function

$$u(y) = u \, \tan\left(2/\delta\right) \ , \tag{20}$$

where u and δ are the velocity component at vertical position and shear layer thickness, respectively. The initial parameters were chosen in such a way to approximate the velocity profile that constitutes in a short distance from the burner nozzle exit. The generated initial flow field was characterized by the turbulent intensity $T_i = 0.05$, shear layer thickness $\delta = 0.5 \times 10^{-3}$ m and the Reynolds number $\mathrm{Re}_\lambda = u'\lambda/\upsilon = 0.8$, where $u' = T_i\, u$ and $\mathrm{Re}_\delta = u\delta/\upsilon = 100$ here υ is the kinematic viscosity. The resulted Kolmogorov length scale for the initial flow field was equal to $\eta_K = 1.092 \times 10^{-5}$ m.

Later in the paper, the cases denoted as 'no-model' label should be not mistaken with DNS results. They refer to the cases without the SGS model. The actual DNS simulation would require a grid refinement. In the current analysis the spatial filter turned out to be greater than the Kolmogorov length scale. In the previous research of the author [7] the results

obtained using different discretization schemes with only single SGS model, using also the denser meshes were compared. It was found that the results showed very similar trends regardless the mesh used.

4 Numerical approach

The numerical procedure used was the implicit LES (ILES) approach. In ILES the SGS scales are modelled along with the chemical source terms $\overline{\dot{\omega}_\alpha(Y,h)}$ assuming $\overline{\dot{\omega}_\alpha(Y,h)} \approx \dot{\omega}_\alpha(\tilde{Y},\tilde{h})$ [6]. The reaction rates are obtained from the Arrhenius formulas applying a one-step chemistry

$$\mathrm{C_2H_5OH} + 3(\mathrm{O_2} + 3.76\,\mathrm{N_2}) \rightarrow 2\mathrm{CO_2} + 3\mathrm{H_2O} + 3 \times 3.76\,\mathrm{N_2}\ , \qquad (21)$$

which minimizes the computational expenses. This simple approach is known for over-predicting the flame speed for rich mixtures as discussed in [4]. Yet it still can reproduce correct trends in the analysis of turbulence impact on the autoignition and flame propagation without resolving the flame speed at all equivalence ratio range in the detail. The ILES is valid for laminar flow simulation and in DNS where all turbulent flow scales are resolved. Hence, one may assume that for sufficiently dense computational meshes, when the grid cells are comparable with the Kolmogorov length scale, the ILES approach is appropriate. This idea was verified in preliminary analyses.

The computations were performed using SAILOR 3D computational fluid dynamics high-order algorithm. The applied code was used and thoroughly verified in previous studies devoted to gaseous flows and flames [20]. The solver is based on the 6th order compact central difference method combined with the projection method for pressure-velocity coupling. The time integration scheme is based on the predictor-corrector approach with the combinations of Adams-Bashforth and Adams-Moulton methods. For solving the equations, governing the dispersed phase motion a 1st order integration is applied. The two-way velocity coupling is realised using 2nd order approximation of momentum source terms with 4th order Lagrangian polynomial approximation of the flow field velocity at the droplet position. The solution procedure was carried out with the varying time-step and the Courant-Friedrichs-Levy number set to CFL= 0.25. Two numerical schemes for the convective term discretization in the species transport equation were used, namely the second-order TVD (total variation diminishing) [21] and fifth-order WENO (weighted essentially nonoscillatory) [22].

5 Results and conclusions

In order to analyse the impact of SGS model on the autoignition process a set of simulations with different SGS models have been performed. The Smagorinsky, Vreman, σ-model and additionally a case without the SGS model were considered, and as mentioned before the last one is referred as 'no-model'. A growth rate of the maximum temperature was acquired and used for comparison of the results. Each flow setup was simulated with the same flow characteristics, i.e., the same Reynolds number and distributions of the velocity fluctuations. The computations started from the same initial conditions and were continued to the moment when an autoignition occurred.

In Figs. 2 and 3 instantaneous values of maximum temperatures inside the domain for different SGS models used, are presented. Surprisingly, for the case with TVD discretization scheme and σ-subgrid model the ignition did not occur even for the long simulation time. This problem is left for further studies.

Analysing the results obtained with the TVD discretization scheme one may observe, that the maximum temperature evolution within the computational domain shows very similar character and seems to be only slightly dependent of SGS model used. The case without any model shows similar behaviour and the reason of that may be attributed to a relatively fine mesh used during the simulations.

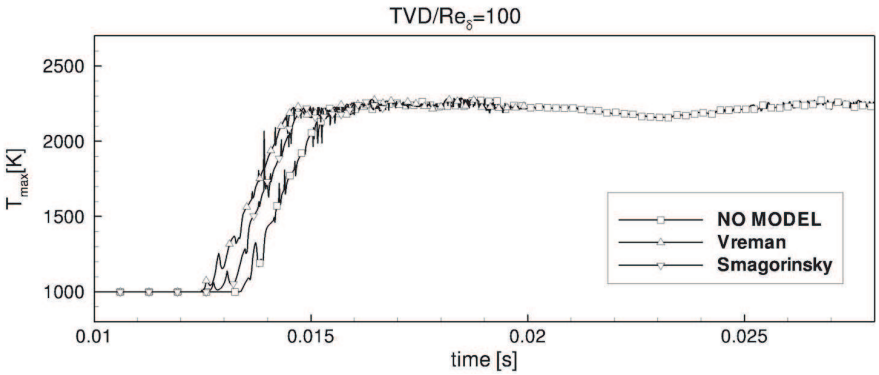

Figure 2: Instantaneous values of maximal temperature inside the domain for different SGS models obtained using the TVD approximation procedure.

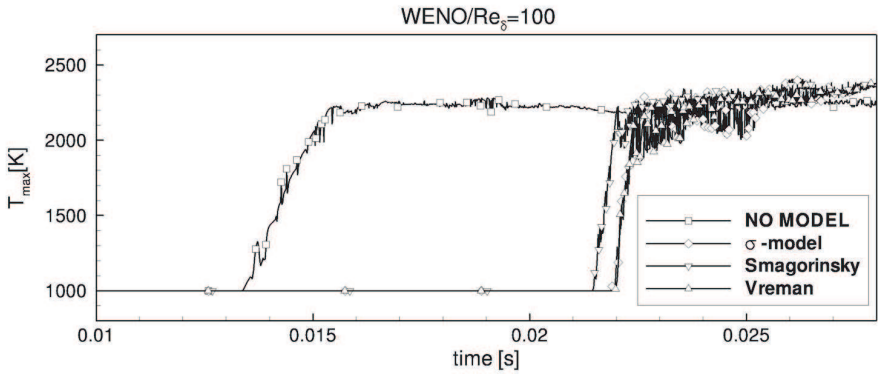

Figure 3: Instantaneous values of maximal temperature inside the domain for different SGS models obtained using the WENO approximation procedure.

Figure 3 shows analogous comparison for the WENO discretization scheme. It can be seen that this time "no-model" case resulted in much faster ignition compared to the cases with SGS model. This is surprising result and it means that for WENO scheme the numerical dissipation interacts with the dissipation introduced by the subgrid viscosity in much more complex way. Application of the Smagorinsky SGS model results in slightly faster ignition than observed for Vreman and σ-model, but the difference is not that significant. Comparing the results from WENO and TVD schemes applied to the 'no-model' case, one may notice that similar ignition times were predicted.

Generally, a strong impact of discretisation scheme is evident comparing the results from both figures. The TVD scheme is known to be more dissipative one. It can be speculated that this property could result in a decrease of the ignition delay since the small flow-scales are not captured but they are damped. The small flow-scales are associated with the short turbulent time-scales and higher turbulence intensities. Their removal leads to a smother ('less turbulent') flow field. It was shown by the others [5] that when the flow is dominated by the small turbulent time-scales, shorter than the laminar autoignition time, the autoignition might be delayed. Hence, as the TVD scheme removes the small scales the opposite effect is observed. One should also consider the fact that the higher order scheme, such as WENO, may introduce numerical oscillations that in general are very difficult to detect. These oscillations could act as small-scale turbulent scales, and thus, contribute to the longer autoignition time.

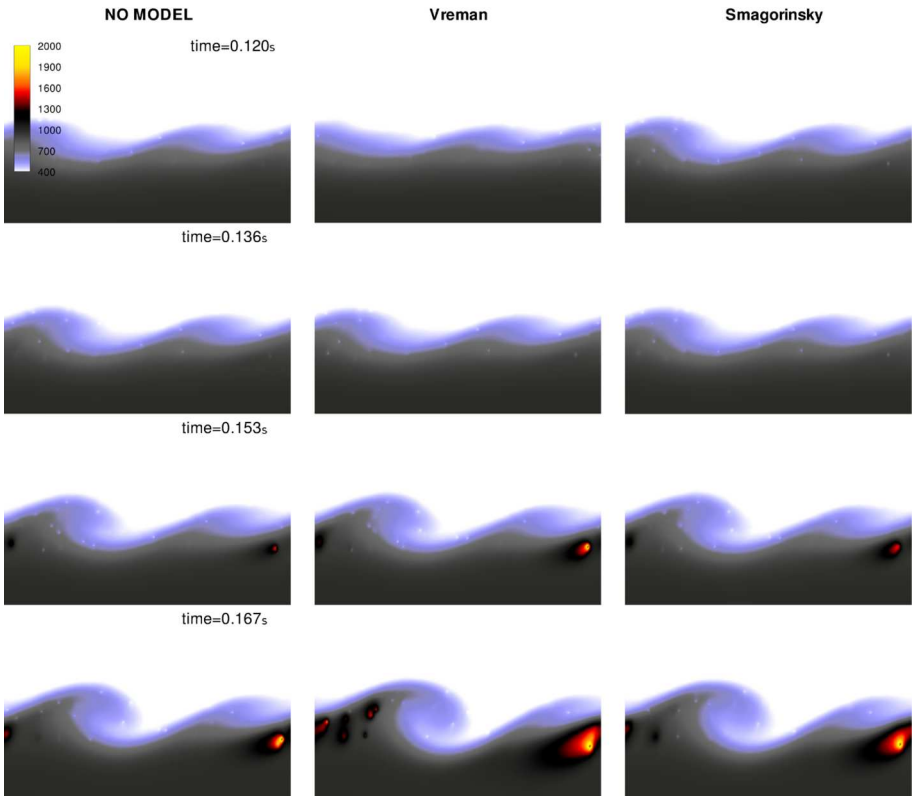

Figure 4: The 2D temperature distribution in the domain section by a z-normal plane obtained for the TVD scheme showing the evolution of the mixing layer and occurrence of ignition spots.

The flame development occurs in the shear layer region where intensive mixing takes place. Figure 4 shows that the results obtained with the use of the TVD scheme reveal slight differences in behaviour of the mixing layer evolution for different SGS models. Although the time evolution of maximum temperature in the domain for different SGS models seems to be very similar (see Fig. 2) the number and localisation of ignition spots vary significantly for different SGS models.

In the case of WENO scheme applied (Fig. 5), the number of ignition spots seems to be similar for every SGS model used. However, the size of the ignition kernel for a given time instance tends to be affected by subgrid modelling. The Smagorinsky model resulted in the biggest ignition kernel whereas σ-model gives the smallest kernel for the same time. The fact that

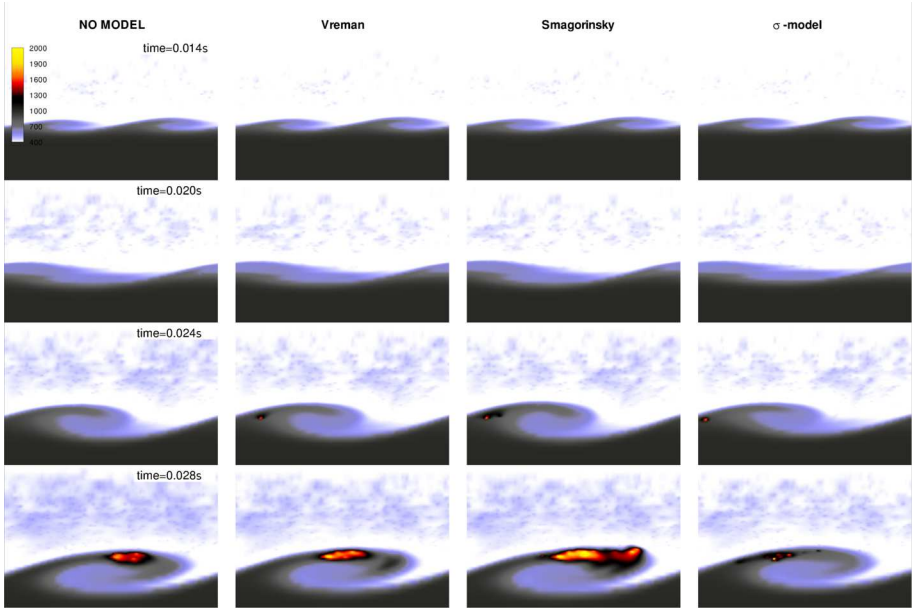

Figure 5: The 2D temperature distribution in a y-x cross-section plane obtained for the WENO scheme showing the evolution of the mixing layer and occurrence of ignition spots.

Smagorinsky SGS model leads to quicker flame growth may results from the dissipative nature of this model.

6 Conclusions

According to the main goal of the study the test of different models and numerical schemes in the LES spray combustion was performed. The simulations were done for the temporal and periodic mixing layer configuration. Hence, the influence of inlet/outlet boundary conditions was eliminated. Significant differences in ignition times were observed comparing the WENO and the TVD schemes. The WENO scheme resulted in much longer autoignition delays. An impact of SGS modelling seemed to be less significant. Especially for TVD scheme where only minor differences were observed even for the case without SGS model. In case of the WENO discretization scheme the impact of SGS model is stronger. The results from the case without SGS model shows similar behaviour as the results with the TVD scheme. However, when the SGS model is applied in combination with

WENO scheme a strong delay in ignition is observed. The autoignition time and the rate of the maximum temperature growth predicted by the LES are significantly affected by the numerics. This is very important message, which shows that the discretisation method can have comparable or even larger impact than the subgrid modelling. Unfortunately, there is a lack of experimental data for the investigated cases to which the numerical results could be compared. Therefore, univocal conclusion about the model accuracy cannot be formulated. The performed analysis emphasizes the importance of numerics and modelling approaches. It was presented that the results depend on the choice of SGS model and discretization method. This indicate also that high caution is required drawing conclusions based on a LES of spray combustion.

Acknowledgments This work was supported by grant 2015/17/B/ST8/03217 (National Science Centre, Poland) and statutory funds BS/PB-1-103-3010/11/P. PL-Grid infrastructure was used to carry out the computations.

Author would like also to express the appreciation to the A. Tyliszczak for discussing some details concerning the numerical issues addressed in the paper. Also, I would like to thank L. Kuban for giving me valuable comments which led to the improvement of the paper's content.

Received 10 May 2017

References

[1] Smagorinsky J.: *General circulation experiments with the primitive equations.* Mon. Wea. **91**(1963), 3, 99–164.

[2] Vreman A.W.: *An eddy-viscosity subgrid-scale model for turbulent shear flow: Algebraic theory and applications.* Phys. Fluids **16**(2004), 4, 3670–3681.

[3] Nicoud F., Toda H. B., Cabrit O., Bose S., Lee J.: *Using singular values to build a subgrid-scale model for large eddy simulations.* Phys. Fluids **23**(2011), 8, 1–12.

[4] Chakraborty N.A., Mastorakos E., Cant S.: *Effects of turbulence on spark ignition in inhomogeneous mixtures: A direct numerical simulation (DNS) study.* Combust. Sci. Technol. **179**(2007), 1-2, 293–317.

[5] Hilbert R. Thevenin D.: *Autoignition of turbulent non-premixed flames investigated using direct numerical simulations.* Combust. Flame **128**(2002), 1-2, 22–37.

[6] Duwig C., Nogenmyr K. J., Chan C., Dunn M. J.: *Large eddy simulations of a piloted lean premix jet flame using finite-rate chemistry.* Combust. Theor. Model. **15**(2011), 4, 537–568.

[7] Stempka J., Kuban L., Bogusławski A., Tyliszczak A.: *DNS and ILES study of ethanol spray auto-ignition in a time-evolving mixing layer.* In: Proc. 8th European Combustion Meeting, Dubrovnik 2017, 1076–1081.

[8] Jaegle F.: *Large eddy simulation of evaporating sprays in complex geometries using Eulerian and Lagrangian methods.* PhD thesis, Institut National Polytechnique de Toulouse – INPT, Toulouse 2009.

[9] Geurts B.: *Elements of direct and large-eddy simulation.* R.T. Edwards, Inc., Philadelphia 2003.

[10] Favre A.: *Turbulence: space-time statistical properties and behaviour in supersonic flows.* Phys. Fluids **26**(1983), 10, 2851–2863.

[11] Jones W.P., Marquis A.J., Vogiatzaki K.: *Large-eddy simulation of spray combustion in a gas turbine combustor.* Combust. Flame **161** (2014), 1, 222–239.

[12] Sagaut P., Deek S., Terracol M.: *Multiscale and Multiresolution Approaches in Turbulence.* Imperial College Press, London 2006.

[13] Tyliszczak A.: *High-order compact difference algorithm on half-staggered meshes for low Mach number flows.* Comput. Fluids **127**(2016), 131–145.

[14] Maxey M. R., Riley J. J.: *Equation of motion for a small rigid sphere in a nonuniform flow.* Phys. Fluids **26**(1983), 4, 883–889.

[15] Spalding D.B.: *Experiments on the burning and extinction of liquid fuel spheres.* Fuel **32**(1953), 169–185.

[16] Abramzon B., Sirignano W.A.: *Droplet vaporization model for spray combustion calculations.* Int. J. Heat Mass Tran. **32**(1989), 9, 1605–1618.

[17] Pino Martin M.: *Subgrid-scalem models for compressible large-eddy simulations.* Theor. Comp Fluid Dyn. **13**(2000), 5, 361–376.

[18] Vreman B., Geurts B., Kuerten H.: *A priori test of large eddy simulation of the compressible turbulence.* J. Eng. Math. **29**(1995), 4, 299–327.

[19] Baya Toda H., Cabrit O., Balarac G., Bose S., Lee J., Choi H., Nicoud F.: *A subgrid-scale model based on singular values for LES in complex geometries.* Centre for Turbulence Research. Proc. Summer Program, 2010, 193–202.

[20] Tyliszczak A.: *Physics of Fluids (1994-present)* Phys. Fluids **27**(2015), 041703.

[21] Hirsch C.: *Numerical Computation of Internal and External Flows.* John Wiley & Sons, New Jersey 2001.

[22] Shu C.W.: *Essentially non-oscillatory and weighted essentially non-oscillatory schemes for hyperbolic conservation laws.* In: Advanced Numerical Approximation of Nonlinear Hyperbolic Equations, 2nd Session of the Centro Internazionale Matematico Estivo (C.I.M.E.), Cetraro, (2006), 325–432.

[23] Kosowska-Golachowska M. Kijo-Kleczkowska A., Luckos A., Wolski K., Musiał T.: *Oxy-combustion of biomass in a circulating fluidized bed.* Arch. Thermodyn. **37**(2016), 1, 17–30.

[24] Ma Z., Chen H., Zhang Y.: *Impact of waste heat recovery systems on energy efficiency improvement of a heavy-duty diesel engine.* Arch. Thermodyn. **38**(2017), 3, 63–75.

[25] Hnydiuk-Stefan A., Składzień J.: *The analysis of parameters of the cryogenic oxygen unit cooperating with power plant to realize oxy-fuel combustion.* Arch. Thermodyn. **36**(2015), 1, 39–54.

[26] Faeth G.M.: *Current status of droplet and liquid combustion.* Prog. Energy Combust. Sci. **3**(1977), 191–224.